Evaluation of Radiocarbon 14C Yield under Conditions of Thunderstorms

Vladimir Lyashuk[1]

[1]Institute for Nuclear Research (INR) of the Russian Academy of Sciences

November 23, 2022

Abstract

The knowledge of the radioactive 14C yield under atmosphere thunderstorm flash conditions (the additional discovered channel of 14C production relative to the main - cosmogenic one) is important for radiocarbon analysis. It is proposed the gross model for evaluation of the thunderstorm 14C yield simulated for the altitudes up to 15 km. It was obtained that yield from the thunderstorm mechanisms of 14C creation cannot compete with cosmogenic production which is six orders of value larger. The obtained result allows to take off the problematic issue on thunderstorm radiocarbon generation in the atmosphere as the additional significant source.

Evaluation of Radiocarbon 14C Yield under Conditions of Thunderstorms

V. I. Lyashuk[1,2]

[1]Institute for Nuclear Research of the Russian Academy of Sciences, Moscow, Russia.

[2]National Research Center "Kurchatov Institute", Moscow, Russia.

Corresponding author: V. I. Lyashuk (lyashuk@itep.ru)

Key Points:

- The gross model for evaluation of the radiocarbon ^{14}C creation at thunderstorms.
- Probability of ^{14}C generation in the atmosphere depending on the neutron energy.
- Radiocarbon yield under thunderstorms at different altitudes.
- Comparison of radiocarbon yield under thunderstorms and from the cosmic irradiation.

Abstract

The knowledge of the radioactive 14C yield under atmosphere thunderstorm flash conditions (the additional discovered channel of 14C production relative to the main - cosmogenic one) is important for radiocarbon analysis. It is proposed the gross model for evaluation of the thunderstorm 14C yield simulated for the altitudes up to 15 km. It was obtained that yield from the thunderstorm mechanisms of 14C creation cannot compete with cosmogenic production which is six orders of value larger. The obtained result allows to take off the problematic issue on thunderstorm radiocarbon generation in the atmosphere as the additional significant source.

Plain Language Summary

The creation of isotopes takes place not only in stellar conditions but also in the Earth atmosphere under cosmic irradiation. Radioactive carbon 14C produced in the atmosphere is exclusively important tool for historical dating (in the archaeology, glaciology, biology, paleontology, geology, Sun activity and climate in the past) for the time scale up to ~ (50-60) thousands of years. But it creation is possible also at the thunderstorm discharge. In case of significant yield it will cause the correction of the dating results. For solving of the problem it was proposed the model which takes into account the rate of 14C production depending on the part of energetic electrons in the thunderstorm flash discharges for different altitudes. It was calculated the probability of 14C creation depending on the energy of neutrons generated under thunderstorms. The results revealed that yield of thunderstorm mechanism is very small compare to the main one originated from the cosmic irradiation. It allows to take off the problematic question on the correction arising from this additional source of 14C isotope. The reliability of the obtained results is confirmed by simulation of the Japan experiment on neutron registration at the strong thunderstorm in 5 Jan., 2012.

1 Introduction

The main mechanism of radiocarbon ^{14}C creation in the Earth atmosphere is ensured by cosmogenic irradiation with yield of 472 g-mole/year (Roth & Joos, 2013) in the reaction ^{14}N(n,p)^{14}C. The generated isotope of ^{14}C is assimilated in the biomass (in the form of CO_2) and decays within it ($T_{1/2}$ = 5700 y) that allows to date the age of the investigated organic materials. Discovery of short-term secular fluctuations of radiocarbon in tree rings (Suess, 1965) and it correlation with number of sun spots had caused questions that should be taken off and the nature of the phenomena must be explained. In addition to solar mechanism of fluctuations it was proposed the hypothesis of short-term ^{14}C variation under thunderstorm neutron fluence (Libby & Lukens, 1973). Synthesis of the isotope ^{14}C under conditions of atmospheric thunderstorms goes at the end of process chain (Babich & Roussel-Duprè, 2007; Babich, 2017a; Babich, 2017b): the electrons in the lightning discharge avalanche slow down and escape *x*-radiation (bremsstrahlung); the escaped *x*-rays produce flux of photo-neutrons in $^{14}N(\gamma,Xn)$-reaction ($E_{threshold}$ = 10.6 MeV), where Xn – emission of X=1, 2 or more neutrons; the produced photo-neutrons slow down creating radiocarbon in $^{14}N(n,p)^{14}C$ –process. For investigating of ^{14}C production at thunderstorms we considered the above mentioned processes and simulated in detail the electron, photon and neutron transport in the model based on MCNPX code (editor: Pelowitz, 2008).

2 The gross model for particle transport simulation in the atmosphere

It were detected many times that electric discharges in the atmosphere are accompanied by gamma flashes and increase of neutron flux (for example: Shan et al., 1985; Shyam & Kaushik, 1999; Chilingarian et al., 2010; Starodubtsev et al., 2012). In 2017 the phenomenon of neutron production in (γ,Xn)-process and creation of isotopes (^{13}C, ^{13}N, ^{15}N, ^{15}O) at thunderstorms were confirmed experimentally that inevitable means the creation of the radiocarbon ^{14}C too (Enoto et al., 2017). As neutron production in the atmosphere is the threshold reaction, the ^{14}C synthesis can be realized only by relativistic electrons with energy higher then threshold one. The energetic electron spectrum in our model is applied as $f \propto \exp(-\varepsilon /7.3\ [\mathrm{MeV}])$ (Dwyer & Babich, 2011) where ε is the energy of the runaway electrons (i.e., electrons accelerated in the electric fields of thunderclouds; the process was investigated by Wilson almost a century ago (Wilson, 1925). The spectrum spreads up to ≃60 MeV ensuring the multiplication of the avalanche under atmospheric electric conditions. Namely relativistic electrons (E >1 MeV) move in the forward part of the lightning discharge generating the low energy electrons in interactions (via ionization of the media), drawing them into the avalanche propagated and accelerated in the thunderstorm electric field. On the contrary the electrons which energy decreases below the threshold (≃ 100 eV) are fall out from the avalanche, forming the dynamical equilibrium between involved and lost electrons. In the avalanche the number of low energy electrons N_{le} strongly exceeds the relativistic ones N_{re} . At the altitude H the minimal relation $R1 = N_{le} / N_{re}$ is equal to

$\simeq(1.3\times10^4)\times n$, where $n=\rho(H)/\rho(H=0)$, $\rho(H)$ - density of the air relative to the sea level (H = 0) (Dwyer & Babich, 2011). So, the total charge of lightning is ensured almost entirely by low energy electrons which part in the avalanche decreases for higher altitudes.

Taking into account the dependence of relation N_{le} / N_{re} from the air density the simulation was realized for the altitudes from the sea level up to the H =15 km (i.e., including the upper charge layer of thunderclouds at typical elevation H=(10÷14) km) (Rakov & Uman, 2005). In the model we use the spherical geometry with centers (the point source of energetic electrons of isotropic f-spectrum) on the indicated altitudes (**Fig. 1**).

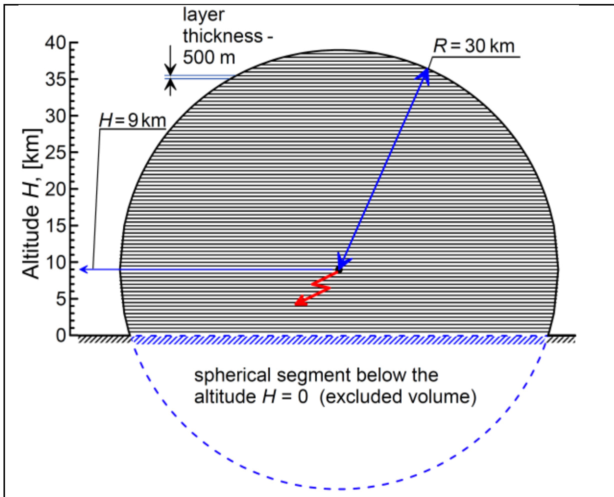

Fig. 1. Geometry of the spherical-layers model for simulation of the particles transport and calculation of radiocarbon ^{14}C creation in the air under conditions of thunderstorms lightning (examples for lightning [indicated as red arrow] origin at the altitude H = 9 km on the sea level). The spherical segment below the sea level (H =0) is excluded from ^{14}C accumulation.

The spheres are divided into horizontal plane layers (of 500 m thickness) with air density ρ corresponding to the layers heights. In order to exclude the escape of the valuable part of neutrons (born in the sphere in (γ,Xn)-process) the sphere radii R were increased up to 30 km that prevent neutron loose and especially important for it high energy spectrum part. As a result the percent of the escaping neutrons had been reduced below 1% of created ones. In addition to neutron generation in interaction with ^{14}N the yields from $^{16}O(\gamma,n)^{15}O$, $^{40}Ar(\gamma,n)^{39}Ar$ reaction was accounted. As a result it was found that ^{14}N, ^{16}O and ^{40}Ar are responsible for production of 75.3%, 15.7% and 9% from the all created neutrons correspondingly. The example of calculated neutron spectrum at H = 10 km compare to the cross section of the $^{14}N(\gamma,Xn)$-reaction is given in the **Fig. 2** where clear visible the coincidence of the maximum in neutron spectrum to maximal cross section at E_γ =23 MeV.

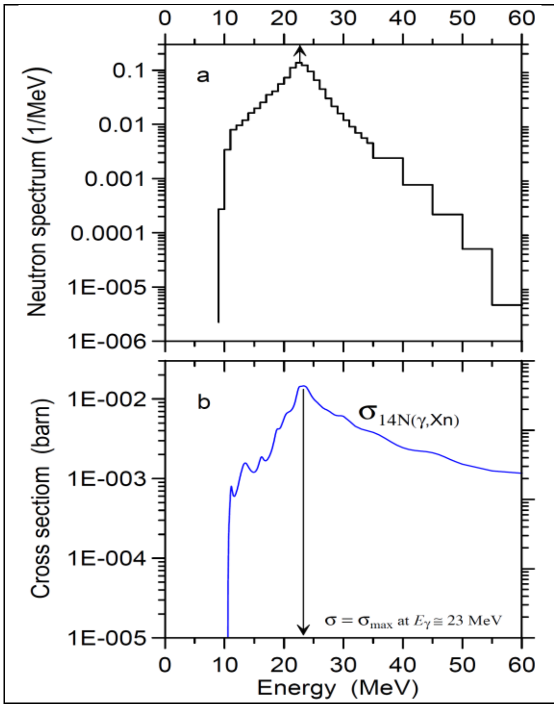

Fig. 2. (a) Spectrum of neutrons produced in the air by (γ,Xn)-process under conditions of thunderstorms lightning. Generation of neutrons is accounted in the reactions: ^{14}N(γ,Xn), ^{16}O(γ,n)^{15}O and ^{40}Ar(γ,n)^{39}Ar. (b) Cross section of the ^{14}N(γ,Xn) photo-neutron production (Shibata et al., 2002) which ensures the main neutron yield. The indicated maximum of the neutron spectrum (arrow at the energy ~ 23 MeV) coincides with maximal cross section at E_γ = 23 MeV.

In this scenario the total number of created neutrons amounts 1.8×10^{10} per 1 coulomb of the flash discharge.

3 Probability of radiocarbon 14N(n,p)14C production

At neutron transport the reaction ^{14}N(n,p)^{14}C of radiocarbon generation competes with processes of neutron captures on the air isotopes which composition is practically stable at change of the altitude H (COESA Working Group, 1976). Then for created neutrons the energy dependence of probability to product the radiocarbon is given by the relation of ^{14}N(n,p)^{14}C macro cross section to the total macro cross section of neutron disappearance (n,disap) in the air:

$$P(E) = \sigma^{macro}_{\mathrm{14N(n,p)14C}}(E) \Big/ \sigma^{macro}_{\mathrm{(n,disap)}}(E) \;, \tag{1}$$

$$\begin{aligned}\sigma^{macro}_{\mathrm{(n,disap)}}(E) = \sum_i \Big[& \sigma^{micro,i}_{(\mathrm{n},\gamma)}(E) + \sigma^{micro,i}_{\mathrm{(n,p)}}(E) + \sigma^{micro,i}_{\mathrm{(n,d)}}(E) + \sigma^{micro,i}_{\mathrm{(n,t)}}(E) + \sigma^{micro,i}_{\mathrm{(n,3He)}}(E) + \\ & \sigma^{micro,i}_{\mathrm{(n,a)}}(E) + \sigma^{micro,i}_{\mathrm{(n,2a)}}(E) + \sigma^{micro,i}_{\mathrm{(n,3a)}}(E) + \sigma^{micro,i}_{\mathrm{(n,2p)}}(E) + \sigma^{micro,i}_{\mathrm{(n,p+a)}}(E) + \\ & \sigma^{micro,i}_{\mathrm{(n,t+2a)}}(E) + \sigma^{micro,i}_{\mathrm{(n,d+2a)}}(E) + \sigma^{micro,i}_{\mathrm{(n,p+d)}}(E) + \sigma^{micro,i}_{\mathrm{(n,p+t)}}(E) + \sigma^{micro,i}_{\mathrm{(n,d+a)}}(E) \Big) \times n_i \Big],\end{aligned} \tag{2}$$

where: $\sigma^{macro}_{\mathrm{14N(n,p)C14}}(E) = \sigma^{micro}_{\mathrm{14N(n,p)C14}}(E) \times n_{\mathrm{14N}}$, $\sigma^{micro}_{\mathrm{14N(n,p)14C}}(E)$ - micro cross sections of

$^{14}N(n,p)^{14}C$ process, n_{14N} - nuclear concentration of ^{14}N isotope. Macro cross section of neutron disappearance in the air is calculated as the sums of indicated micro cross sections (of the reactions leading to neutron disappearance) for the *i*-th isotope multiplied by it nuclear concentration n_i. Owing to the stable air composition for calculation of probability $P(E)$ the isotope concentration can be taken at the sea level $H = 0$.

The behavior of micro cross sections (for all channels of neutron disappearance and (n,disap) - sum of these channels) from the energy for the main air isotopes ^{14}N, ^{16}O and also ^{40}Ar (with 78.14%, 21.03% and 0.47% yield to the total nuclear concentration correspondingly) are presented in the **Fig. 3** (a, b, c) for the energy interval from 60 MeV down to 0.01 eV (i.e., covering the all possible energies of neutrons production and them slow down to thermalization and absorption). The probability of radiocarbon production is strongly depend on the neutron energy and competitive reactions.

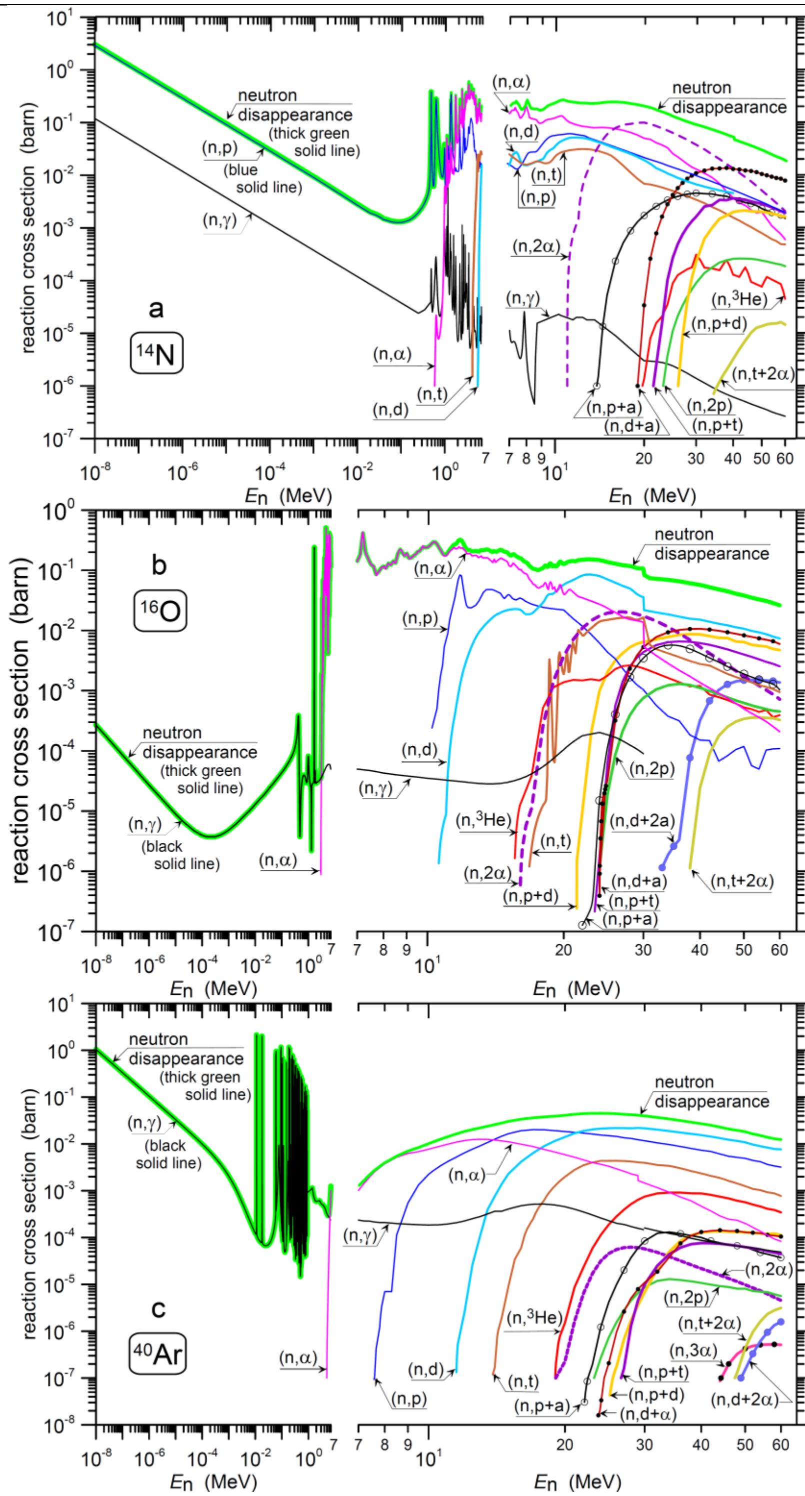

Fig. 3 (a, b, c). Dependence of the (n, disappearance)-micro cross sections from the energy for the nitrogen ^{14}N, oxygen ^{16}O and argon ^{40}Ar. The sum of (n, disap) micro cross section is shown by thick green line. For visualization the dependencies are given in two energy scales with break at E_n= 7 MeV. The sources of the cross sections are given in Table A.1.

At the energy $E_n \gtrsim 1$ MeV the threshold reactions (with yield of a, d, t-particles) go with significant cross sections [see **Fig. 4** (a, b, c)]. In the energy intervals ~ (0.3 ÷ 7) MeV for ^{14}N, ~ (0.4 ÷ 7) MeV for ^{16}O and ~ (0.01 ÷ 1) MeV for ^{40}Ar the cross sections are described by strong resonances [in reactions: (n,p), (n,a) and (n,γ) for ^{14}N; (n,γ) and (n,a) for ^{16}O; (n,γ) for ^{40}Ar] which can be can be carefully processed by resonance integrals in multigroup method used for neutron transport. Below the resonance regions (at energies: $E_n \lesssim 1\times10^{-1}$ MeV for ^{14}N, $E_n \lesssim 1\times10^{-4}$ MeV for ^{16}O and $E_n \lesssim 1\times10^{-3}$ MeV for ^{40}Ar) the cross sections of neutron disappearance reactions [(n,p) and (n,γ) for ^{14}N; (n,γ) for ^{16}O and ^{40}Ar] follow to $1/\upsilon$ low (where υ – neutron velocity), but yield of ^{14}N(n,p)-process strongly dominates in total neutron disappearance in air.

With good precision it is possible to consider the probability to product the radiocarbon as

$$P(E) = \sigma^{macro}_{14\mathrm{N(n,p)14C}}(E) \Big/ \left[\sigma^{macro}_{14\mathrm{N(n,\,disap)}}(E) + \sigma^{macro}_{16\mathrm{O(n,disap)}}(E) + \sigma^{macro}_{40\mathrm{Ar(n,disap)}}(E)\right]. \tag{3}$$

The macro cross cross section of ^{14}N(n,p) reaction, macro cross sections of neutron disappearance in reactions with ^{14}N, ^{16}O and ^{40}Ar (as the main air isotopes) are presented in the **Fig. 4** (a) and **Fig. 4** (b) for the altitude $H = 0$. The summary macro cross section of these main isotopes is indicated in the **Fig. 4** (c) as the $\sigma^{macro}_{\mathrm{(n,disap)}}(\mathrm{Air})$. It is obtained that at the energy $E_n \lesssim 1$ MeV the main yield to the (n,disap)-macro cross section of air is ensured by ^{14}N(n,p)-reaction [see **Fig. 4** (c)]. But at the $E_n \gtrsim 1$ MeV (the energy region of resonances and threshold reactions) the $\sigma^{macro}_{14\mathrm{N(n,p)14}C}$ are lower than $\sigma^{macro}_{disap}(\mathrm{Air})$ from several times to order of value. The precise relation of probability $P(E)$ to product the radiocarbon ^{14}C is given in the **Fig. 4** (d). At the energy $E_n \lesssim 1$ MeV the P-values lay within ~(0.96÷1)-interval and strongly decrease down to P ~ 0.1 at larger energies.

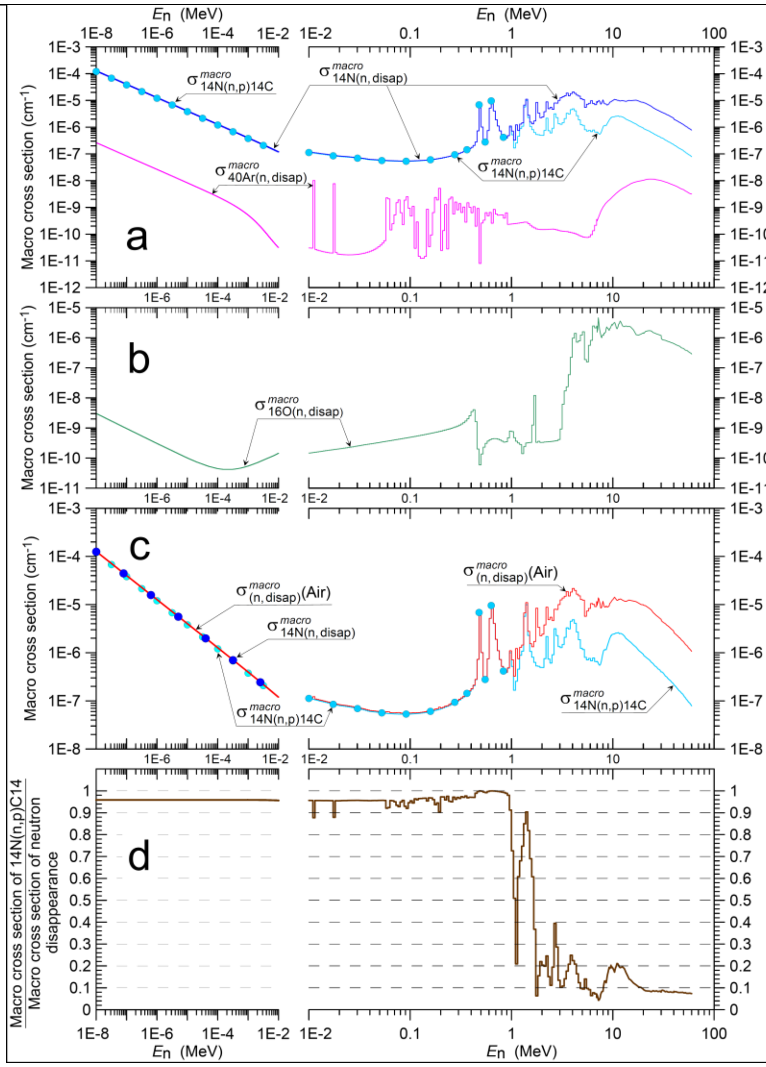

Fig. 4. **(a)** Dependence of (n, disappearance)-macro cross sections of the air isotopes (^{14}N and ^{40}Ar) from the energy (dark blue and violet solid lines correspondingly). Dependence of macro cross section for radiocarbon creation ^{14}N(n,p)^{14}C from the energy (light blue circles ● - at $E_n \lesssim 0.85$ MeV and light blue solid line at $E_n \gtrsim 0.85$ MeV). **(b)** Dependence of (n, disap)-macro cross section of the air isotope ^{16}O from the energy (solid lines). **(c)** Dependence of the summary (n, disap)-macro cross section of the air isotopes (^{14}N, ^{16}O and ^{40}Ar) from the energy is denoted as $\sigma^{macro}_{disap}(\mathrm{Air})$ (red solid lines). Dependence of macro cross section for ^{14}N(n,p)^{14}C-reaction from the energy (light blue circles ● - at $E_n \lesssim 0.85$ MeV and light blue solid line at $E_n \gtrsim 0.85$ MeV). Dependence of $\sigma^{macro}_{14\mathrm{N(n,disap)}}$-macro cross section is shown as dark blue circles ● at the $E_n \lesssim 0.01$ MeV. **(d)** Dependence of the realation $\sigma^{macro}_{14\mathrm{N(n,p)14C}}$ to the $\sigma^{macro}_{disap}(\mathrm{Air})$ from the energy. The all macro cross sections (in the **a**-, **b**-, **c**- and **d**-figures) are given for the altitude H=0 at the sea level. In the figures for better visualization the dependencies are given in two energy scales.

156

4 Evaluation of the radiocarbon ^{14}C yield. Results

At calculation of radiocarbon ^{14}C yield the volumes of the spherical segments below H = 0 (dashed line in the **Fig. 1**) are excluded from the considered volumes. Such a spherical-plane-layers formalism allowed to specify the fraction N_{re} / (N_{le} + N_{re}) of relativistic electrons N_{re} (responsible for ^{14}C production for the current altitude H) in the total (N_{le} + N_{re})-flux and to obtain the ^{14}C yields depending on the altitudes (see **Fig.5**).

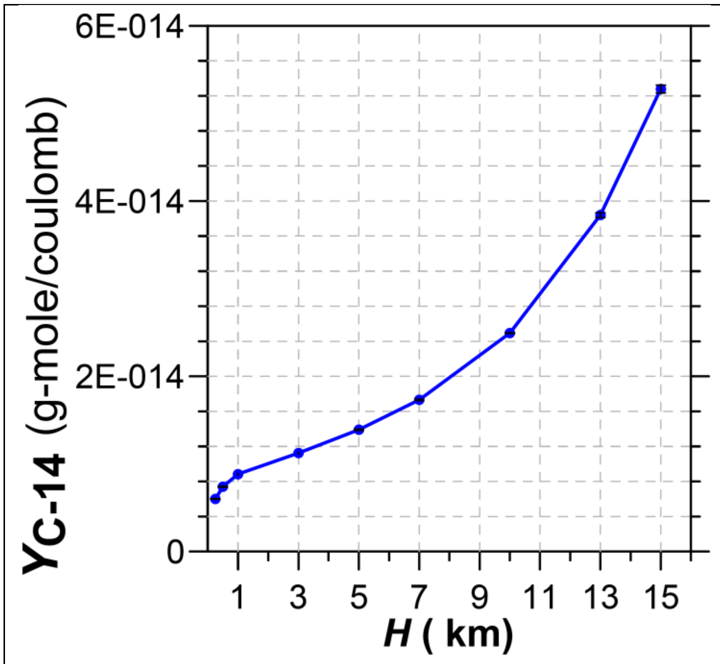

Fig. 5. Yields of radiocarbon ^{14}C depending on the altitude H (km) under thunderstorm conditions. The yields (in gramme-molecules) correspond to one coulomb of lightning discharge. The yields correspond to the electron avalanche model of the work (Dwyer & Babich, 2011) of the lightning discharge.

The $^{14}N(n,p)\,^{14}C$ radiocarbon yields are ensured by part P_{escape} of neutrons which escape the disappearance in the other (n,disap)-reactions [indicated in the Eq. (2), **Fig. 3** (a,b,c)]. So, for the altitude H=10 km it was obtained that P_{escape} = 0.83.

The drop of the low energy population N_{le} in the avalanche at increase of the altitude ensures rise of ^{14}C yield (for the equal lightning charges values). The all presented results of isotope generation (in gramme-molecules) are normalized on the flash charge 1 coulomb. If the discharge occurs between thunderclouds in the horizontal layer (included in the model geometry; see **Fig. 1**) at the some altitude H_{fix} , then the normalized yield corresponds to the function $Y(H_{\mathrm{fix}})$ in the **Fig.5**. In the model the discharge within the horizontal layer can be presented as "movement" of the geometry-model-sphere in the same direction (as discharge movement), that for the indicated task (^{14}C yield evaluation) is equivalently to the fix position of this sphere at the altitude of the discharge. In common case the discharge propagates between some altitudes H_1 and H_2. Then the ^{14}C yield is calculated as the integral along the discharge path S: $Y=\int_S p(x,y,H)\,ds$, where $p(x,y,H)$ is the density of radiocarbon generation at the discharge in the (x,y,H)-coordinates, which depend on the time t as parameter (i.e., $p(x,y,H)\equiv p[x(t),y(t),H(t)]$). If to assume that $[N_{re} / (N_{le} + N_{re})]$ depend only from the altitude H, (i.e., this relation is stable in time and the condition for discharges does not change in x-y –plane), then $p[x(t),y(t),H(t)]=p[H(t)]$. As a result the ^{14}C yield is calculated as $Y=\int_{\Delta t} p[H(t)]dt$ during the discharge time Δt. For the discharge propagated between altitudes H_1 and H_2 (where $H_2 > H_1$) the radiocarbon yield Y will be:

$$Y(H_1)=\int_{\Delta t} p[H_1]dt \ < \ Y < \ Y(H_2)=\int_{\Delta t} p[H_2]dt \ . \tag{4}$$

Let us evaluate the ^{14}C production per year under the lightning conditions (using the data of Fig.5; knowing that the number of lightning on the Earth per 1 year is 1.4×10^9 (Christian et al., 2003); considering that the average lightning charge is ~ 20 coulombs (Rakov & Uman, 2005); allowing the mean altitude of thunderclouds $H\simeq7$ km (Rakov & Uman, 2005). Then Y^{R1}_{C-14} (g-mole/year) $\simeq 1.7\times10^{-14}\times20\times1.4\times10^9 \simeq 5\times10^{-4}$ for the relation $R1$.

Similarly it was simulated and obtained the yield of radioactive ^{41}Ar produced in air (simultaneously with ^{14}C) at neutron activation of the argon ^{40}Ar(n,γ)^{41}Ar. It creation per mean flash (20 coulomb) is Y^{R1}_{Ar-41}(g-mole) $\simeq 2.9\times10^{-17}\times20 \simeq 5.8\times10^{-16}$ for $R1$ value. Owing to relevant ^{41}Ar decay parameters ($T_{1/2}$ = 109.34 m, β^- (100%)) it will be attractive to the consider this isotope as an appropriate tracer of the radiocarbon ^{14}C generation. In spite of debugged technique of ^{41}Ar monitoring (for example on the accelerators and reactors (Cicoria et al., 2017; Oyama et al., 2021) the detection of such low and changing ^{41}Ar concentration is a very complicated task. But it is possible that the detection will be more realistic in case of gigantic terrestial gamma flashes – the large-scale atmospheric phenomena in which population of neutrons exceeds the ~ 10^{15} level (Babich, 2006).

4.1 View on the results n1. Could the radiocarbon yield be strongly larger ?

The obtained yields of ^{14}C is evaluated basing on the relation value $R1\simeq1.3\times10^4$ (Dwyer & Babich, 2011). Today where are two principal scenarios of electron avalanche of the (Dwyer &

Babich, 2011**;** Gurevich et al., 2006). According to the alternative scenario of the electron avalanche (Gurevich et al., 2006) the relation value is $R2 \simeq 3\times10^{6}$ that is more than in the work of (Dwyer & Babich, 2011) by factor of two orders $k = 3\times10^{6}/1.3\times10^{4}$ (see also comments in the Refs.(Gurevich, 2012) and (Dwyer & Babich, 2012) that means decrease of above obtained production in k times: Y^{R2}_{C-14} is equal to Y^{R1}_{C-14}/k and can be considered as the lower limit of ^{14}C yields. On the contrary the Y^{R1}_{C-14} value corresponds to the upper limits of radiocarbon ^{14}C creation.

Compare to the cosmogenic radiocarbon creation the obtained ^{14}C yield under thunderstorm conditions is small: it part is equal to $472/(5\times10^{-4})\simeq1\times10^{-6}$ for 20-coulomb-charge of flashes. An unimportance of thunderstorm ^{14}C yield is agreed also with increase of radiocarbon in tree rings in the time distance AD 774–775 at intensive Sun activity (Miyake et al., 2012). Indeed in case of large ^{14}C yield under conditions of thunderstorms the events with rise of tree-ring-radiocarbon will be smeared and yields from thunderstorms and Sun will be competed. But the solar particles ensure only about 0.25% from the global radiocarbon creation (Kovaltsov et al., 2012) that confirms an insignificance of ^{14}C yield at thunderstorms.

4.2 View on the results n2. Comparison with the experiment

With purpose to test the results of neutron creation, neutron transport (as a key mechanism of ^{14}C generation) it is important to compare the radiation transport results with events of correlated excess for neutron fluxes in case of thunderstorms. At thunder activity at the Ohi Power Station (near Japan sea) the detector PANDA36 had registrated three strong radiation events and one of them (burst-20120105) was correlated with excess of neutron counts (Kuroda et al., 2016). To reproduce the burst sources the authors simulated the events at the combination of height H: 100, 500, 900 and 1300 m (Kuroda et al., 2016). For evaluation of the possible altitudes of the event similar to neutron burst 20120105 (i.e., with the same neutron excess during the time duration 16 s (Kuroda et al., 2016) it was calculated neutron fluences at the ground level (with polar angle of registration $\pi/2$) from the sources at H = 300, 500, 650, 800, 1000 and 1300 m above the sea level. The obtained fluences are normalized on the coulomb of the discharge (see left vertical axis of **Fig. 6**). The right vertical axis of **Fig. 6** shows the expected total counts in case of the detector efficiency 3.15%. The results are in general agreement (or at least in rough agreement) with experimental results.

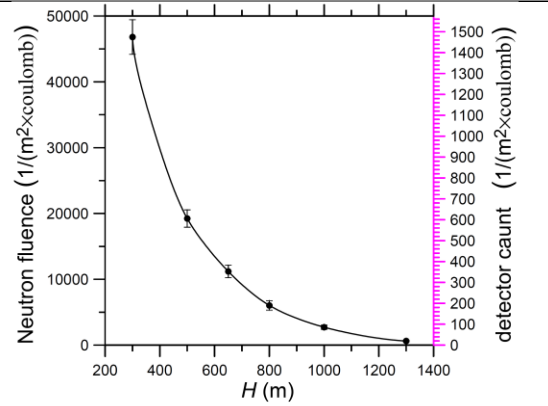

Fig. 6. Dependence of neutron fluences on the ground level (10 m above the sea level) from the altitude H of the lightning discharge (see left vertical axis). Simulation of neutron fluences is realized for the ground position for polar angle of registration $\pi/2$ (at the nadir point in the strict sense). The fluences correspond to one coulomb discharge. The number of expected counts per 1 square meter in the detector (with efficiency 0.0315) is given on the right axis.

So, for example, the neutron excess of ~260 events (as in burst-20120105) can be registrated from ~1.5 coulomb discharge at the altitude H = 800 m or at H = 1 km in case of 3 coulomb discharge. Note that in the report (Kato, 2015) the authors indicated the probable height 400 m for the burst 20120105.

5 Conclusions

It was proposed the gross model for evaluation of the radiocarbon ^{14}C yield under conditions of thunderstorm and simulated it generation depending on the altitude up to 15 km above the sea level. The obtained results allow to conclude that in case of the relation $R1 \simeq 10^4$ of low energy electrons N_{le} to the relativistic ones N_{re} in the discharge avalanche (according to the avalanche scenario of (Dwyer & Babich, 2011) the yield of ^{14}C isotope under thunderstorms adds up to 1×10^{-4} % to the radiocarbon creation from the cosmogenic irradiation that can be considered as upper limit of radiocarbon production from thunderstorm flashes. In the alternative scenario of the relation $R2 = N_{le} / N_{re} \simeq 3\times10^6$ (of the work (Gurevich et al., 2006) the yield of ^{14}C isotope will be in two orders less. The considered scenarios of ^{14}C production indicate on negligible contribution of the thunderstorm radiocarbon to the total creation in the Earth atmosphere that allows to take off the problematic issue on the dating correction caused by the thunderstorm mechanism.

Acknowledgments. Data.

- The author tender thanks to I. N. Borzov for helpful and useful discussion.
- The nuclear data (see Fig.3, Table A.1) are accessible in https://www.oecd-nea.org/janisweb/search/endf , https://www.nndc.bnl.gov/sigma/ and in repositorium https://data.mendeley.com/datasets/dktf9fkwdb/1 , doi: 10.17632/dktf9fkwdb.1

Appendix A

The cross sections for the reactions leading to neutron disappearance on the 14N, 16O and 40Ar isotopes and sum of these channels are presented in the **Fig. 3** (a, b, c). The nuclear data libraries used for these plots are indicated in the Table A.1.

Table A.1. Reaction of neutron disappearance on the isotopes of ^{14}N, ^{16}O, ^{40}Ar [in the Fig. 3 (a, b, c)] and international nuclear data libraries (EAF-2010: Sublet et al., 2010; ENDF/B-VIII: Brown et al., 2018; TENDL-2019 and 2009: Koning et al., 2019; JEFF-3.0: EOCD/NEA Data Bank, 2005) used for the total E < 60 MeV interval or for indicated intervals of neutron energy. The reaction numbers MT correspond to the ENDF-6 format (editors: Herman & Trkov, 2009).

MT[a]	reaction	^{14}N	^{16}O	^{40}Ar
101	(n,disap)	No data	No data	No data
102	(n,γ)	EAF-2010	*E* < 30 MeV, ENDF/B-VIII	TENDL-2019
103	(n,p)	*E* < 20 MeV, ENDF/B-VIII. *E* = (20-60) MeV, EAF-2010	EAF-2010	TENDL-2009
104	(n,d)	*E* < 20 MeV, ENDF/B-VIII. *E* = (20-40) MeV, JEFF-3.0	*E* < 30 MeV, ENDF/B-VIII E = (30-60) MeV, EAF-2010	EAF-2010
105	(n,t)	*E* < 20 MeV, ENDF/B-VIII. *E* = (20-60) MeV] EAF-2010	*E* < 30 MeV, ENDF/B-VIII. *E* = (30-60) MeV, EAF-2010	TENDL-2009
106	(n,^{3}He)	TENDL-2009	EAF-2010	EAF-2010
107	(n,a)	TENDL-2019	*E* < 30 MeV, ENDF/B-VIII. *E* = (30-60) MeV, EAF-2010	*E* < 29 MeV, TENDL-2019. *E* > 29 MeV, EAF-2010
108	(n,2a)	EAF-2010	EAF-2010	EAF-2010
109	(n,3a)	No data	No data	EAF-2010
111	(n,2p)	EAF-2010	EAF-2010	— / —
112	(n,p+a)	— / —	— / —	— / —
113	(n,t+2a)	— / —	— / —	— / —
114	(n,d+2a)	No data	— / —	— / —
115	(n,p+d)	EAF-2010	— / —	— / —
116	(n,p+t)	— / —	— / —	— / —
117	(n,d+a)	— / —	— / —	— / —

[a] MT=101 is the sum of the neutron disappearance reactions (sum of MT=102— 117). MT=101 is used very rarely. MT=110 is not used in ENDF-6 format.

References

Babich, L.P. (2006). Generation of neutrons in giant upward atmospheric discharges, *Jetp Lett.*, 84, 285-288. https://doi.org/10.1134/S0021364006180020

Babich, L.P., Roussel-Duprè, R.A. (2007). Origin of neutron flux increases observed in correlation with lightning. *J. Geophys. Res.: Atmospheres* **112**, D13303. https://doi.org/10.1029/2006JD008340.

Babich, L.P. (2017)a. Radiocarbon Production by Thunderstorms. *Geophysical Research Letters*, 44, pp.11,191-11,200. https://doi.org/10.1002/2017GL075131

Babich, L.P. (2017)b. Thunderous nuclear reactions. *Nature*, 551, 443-444. https://doi.org/10.1038/d41586-017-07266-w

Brown, D.A., Chadwick, M.B., Capote, R., Kahler, A.C., Trkov, A., Herman, M.W., Sonzogni, A.A., Danon, Y., Carlson, A.D., Dunn, M., Smith, D.L., Hale, G.M. Arbanas, G., Arcilla, R., Bates, C.R., Beck, B., Becker, B., Brown, F., Casperson, R.J., Conlin, J., Cullen, D.E., Descalle, M.-A., Firestone, R., Gaines, T., Guber, K.H., Hawari, A.I. Holmes, J., Johnson, T.D., Kawano, T., Kiedrowski, B.C. Koning, A.J., Kopecky, S., Leal, L., Lestone, J.P., Lubitz, C., Márquez Damián, J.I., Mattoon, C.M., McCutchan, E.A., Mughabghab, S., Navratil, Neudecker, P.D., Nobre, G.P.A., Noguere, G., Paris, M., Pigni, M.T. Plompen, A.J., Pritychenko, B., Pronyaev, V.G., Roubtsov, D., Rochman, D., Romano, P., Schillebeeckx, P., Simakov, S., Sirakov, M.Sin, I., Sleaford, B., Sobes, V., Soukhovitskii, E.S., Stetcu, I., Talou, P., Thompson, I., Van Der Marck, S., Welser-Sherrill, L., Wiarda, D., White, M., Wormald, J.L., Wright, R.Q., Zerkle, M., Žerovnik, G., Zhu, Y. (2018). ENDF/B-VIII.0: The 8th major release of the nuclear reaction data library with CIELO-project cross sections, new standards and thermal scattering data. *Nucl. Data Sheets*, **148,** 1-142. https://doi.org/10.1016/j.nds.2018.02.001

Chilingarian, A., Daryan, A., Arakelyan, K., Hovhannisyan, A., Mailyan, B., Melkumyan, L., Hovsepyan, G., Chilingaryan, S., Reymers, A., Vanyan, L. (2010). Ground-based observations of thunderstorm-correlated fluxes of high-energy electrons, gamma rays, and neutrons. *Phys. Rev. D*, 82, 043009. https://doi.org/10.1103/PhysRevD.82.043009

Christian, H.J., Blakeslee, R.J., Boccippio, D.J., Boeck, W.L., Buechler, D.E., Driscoll, K.T., Goodman, S.J., Hall, J.M., Koshak, W.J., Mach D.M., Stewart, M.F. (2003). Global frequency and distribution of lightning as observed from space by the Optical Transient Detector. *J. Geophys. Res.: Atmospheres*, 108, ACL 4-1-ACL 4-15. https://doi.org/10.1029/2002JD002347

Cicoria, G., Cesarini, F., Infantino, A., Vichi, S., Zagni, F., Marengo, M. (2017). Characterization of 41Ar production in air at a PET cyclotron facility. *Modern Phys. Lett. A*, 32 (17), 1740014-1 - 1740014-14. https://doi.org/10.1142/S0217732317400144

COESA Working Group, NASA-TM-X-74335. U.S. Standard atmosphere, (1976) (National Aeronatic and Space Administration). Retrieved from https://www.ngdc.noaa.gov/stp/space-weather/online-publications/miscellaneous/us-standard-atmosphere-1976/us-standard-atmosphere_st76-1562_noaa.pdf.

Dwyer, J.R., Babich, L.P. (2011). Low-energy electron production by relativistic runaway electron avalanches in air. *J Geophys. Res.: Sp. Phys.*, 116, A09301. https://doi.org/10.1029/2011JA016494

Dwyer, J.R., Babich, L.P. (2012). Reply to comment by A. V. Gurevich et al. on “Low-energy electron production by relativistic runaway electron avalanches in air”. *J. Geophys. Res.: Sp. Phys.*, 117, A04303. https://doi.org/10.1029/2011JA017487

ENDF-6 Formats Manual. Data Formats and Procedures for the Evaluated Nuclear Data FilesENDF/B-VI and ENDF/B-VII. CSEWG Document ENDF-102. Written by the Members of the Cross Sections Evaluation Working Group Edited by M. Herman and A. Trkov. (June 2009). National Nuclear Data Center Brookhaven National Laboratory. Upton, NY 11973-5000). Retrieved from https://www.oecd-nea.org/dbdata/data/manual-endf/endf102.pdf.

Enoto, T., Wada, Y., Furuta, Y., Nakazawa, K., Yuasa, T., Okuda, K., Makishima, K., Sato, M., Sato, Y., Nakano, T., D. Umemoto, D., Tsuchiya, H. (2017). Photonuclear reactions triggered by lightning discharge. *Nature*, 551, 481-484. https://doi.org/10.1038/nature24630

Gurevich, A.V., Zybin K.P., Yu.V. Medvedev, Yu.V. (2006). Amplification and nonlinear modification of runaway breakdown. *Phys. Lett. A*, 349, 331-339. https://doi.org/10.1016/j.physleta.2005.09.074

Gurevich, A.V., Roussel-Dupre, R., Zybin, K.P., Milikh, G.M. (2012). Comment on “Low-energy electron production by relativistic runway electron avalanches in air” by J. R. Dwyer and L. P. Babich. *J. Geoph. Res.: Sp. Phys.*, 117, A04302. https://doi.org/10.1029/2011JA017431

Kato, Y. (2015). Thundercloud-related radiation bursts observed at a coastal area and a mountaintop using a segmented organic scintillators. Presented at International Symposium at the Yerevan Physics Institute (TEPA-2015), October 5-9, 2015, Yerevan Physics Institute, Byurakan, Aragatsotn District, Armenia. Retrieved from http://crd.yerphi.am/Conferences/tepa2015/files/presentations/Oct7/20151007_TEPA2015_ykato.pdf.

Koning, A.J., Rochman, D., Sublet, J., Dzysiuk, N., Fleming M., van der Marck, S. (2019). TENDL: Complete Nuclear Data Library for Innovative Nuclear Science and Technology. *Nucl. Data Sheets*, 155, 1-55. https://doi.org/10.1016/j.nds.2019.01.002

Kovaltsov, G.A., Mishev, A., Usoskin, I.G. (2012). A new model of cosmogenic production of radiocarbon 14C in the atmosphere. *Earth and Planetary Science Lett.*, 337-338, 114-120. https://doi.org/10.1016/j.epsl.2012.05.036

Kuroda, Y., Oguri, S., Kato, Y., Nakata, R., Inoue, Y., Ito, C., Minowa, M. (2016). Observation of gamma ray bursts at ground level under the thunderclouds. *Phys. Lett. B*, 758, 286-291. https://doi.org/10.1016/j.physletb.2016.05.029

Libby, L.M., Lukens, H.R. (1973). Production of radiocarbon in tree rings by lightning bolts. *J. Geophys. Res.*, 78, 5902-5903. https://doi.org/10.1029/JB078i026p05902

MCNPX User's Manual (LA-CP-07-1473), Version 2.6.0, Denise B. Pelowitz, editor (2008). Retrieved from https://manualzz.com/doc/7250495/mcnpx.

Miyake, F., Nagaya, K., Masuda, K., Nakamura, T. (2012). A signature of cosmic-ray increase in ad 774–775 from tree rings in Japan. *Nature*, 486, 240-242. https://doi.org/10.1038/nature11123

Los Alamos National Lab., http://www.njoy21.io/. Retrieved from http://www.njoy21.io/

OECD/NEA Data Bank, (2005). The JEFF-3.0 Nuclear Data Library. JEFF Report 19, OECD/NEA Data Bank (2005). Retrieved from https://www.oecd-nea.org/jcms/pl_14080.

Oyama, T., Nagaguro, S., Hagiwara, M., Nakamura, H., Shirakata, M., Saito, K., Yamazaki H. (2021). Measurements and Characterization of Air Activation in J-PARC Main Ring. *JPS Conf. Proc.*, 011147-1 - 011147-6. https://doi.org/10.7566/JPSCP.33.011147

Rakov, V.A., Uman, M.A. (2005). Lightning: Physics and Effects, Cambridge Univ. Press, Cambridge. ISBN: 9780521035415.

Roth, R., Joos F. (2013). A reconstruction of radiocarbon production and total solar irradiance from the Holocene 14C and CO2 records: implications of data and model uncertainties. *Clim. Past*, 9, 1879-1909. https:/doi.org/10.5194/cp-9-1879-2013

Shan, G.N., Razdan, H., Blat, C.L., Ali, Q.M. (1985). Neutron generation in lightning bolts.

Nature, 313, 773-775. https://doi.org/10.1038/313773a0

Shibata, K., Kawano, T., Nakagawa, T., Iwamoto, O., Katakura, J., Fukahori, T., Chiba, S., Hasegawa, A., Murata, T., Matsunobu, H., Ohsawa, T., Nakajima, Y., Yoshida, T., Zukeran, A., Kawai, M., Baba, M., Ishikawa, M., Asami, T., Watanabe, T., Watanabe, Y., Igashira, M., Yamamuro, N., Kitazawa, H., Yamano N., and Takano, H. (2002). Japanese Evaluated Nuclear Data Library Version 3 Revision-3: JENDL-3.3. *J. Nucl. Sci. Technol.*, 39, 1125. https://doi.org/10.1080/18811248.2002.9715303

Shyam A., Kaushik, T.C. (1999). Observation of neutron bursts associated with atmospheric lightning discharge. *J. Geophys. Res.: Sp. Phys.*, 104, 6867-6869. https://doi.org/10.1029/98JA02683

Starodubtsev, S.A., Kozlov, V.I., Toropov, A.A., Mullayarov, V.A., Grigor'ev, V.G., Moiseev, A.V. (2012). First experimental observations of neutron bursts under thunderstorm clouds near sea level. *JETP Lett.*, 96, 188-191. https://doi.org/10.1134/S0021364012150106

Sublet, J.-Ch., Packer, L.W., Kopecky, J., Forrest, R.A., Koning, A. J., Rochman, D.A. (2010). The European Activation File: EAF-2010 neutron-induced cross section library. EASY Documentation Series. CCFE-R (10) 05. 2010. Retrieved from https://t2.lanl.gov/nis/data/jeff/EAF2010.pdf.

Suess, H.E. (1965). Secular variations of the cosmic-ray-produced carbon 14 in the atmosphere and their interpretations. *J. Geophys. Res.*, 70, 5937-5952. https://doi.org/10.1029/JZ070i023p05937

Wilson, C.T.R. (1925). The Acceleration of β-particles in Strong Electric Fields such as those of Thunderclouds. Math. *Proc. of the Cambridge Philos. Soc.*, 22, 534-538. https://doi.org/10.1017/S0305004100003236